Plant Cell Reports (2023) 42:165–179
https://doi.org/10.1007/s00299-022-02947-x

ORIGINAL ARTICLE

Inoculation of wheat with *Bacillus* sp. wp-6 altered amino acid and flavonoid metabolism and promoted plant growth

Yaguang Zhao[1] · Fenghua Zhang[1] · Bede Mickan[2] · Dan Wang[1]

Received: 13 July 2022 / Accepted: 29 October 2022 / Published online: 8 November 2022

Abstract

Key message **Inoculation of wheat seedling with *Bacillus* sp. wp-6 changed amino acid metabolism and flavonoid synthesis and promoted plant growth.**

Abstract Plant growth-promoting rhizobacteria (PGPR), which can reduce the use of agrochemicals, is vital for the development of sustainable agriculture. In this study, proteomics and metabolomics analyses were performed to investigate the effects of inoculation with a PGPR, *Bacillus* sp. wp-6, on wheat (*Triticum aestivum* L.) seedling growth. The results showed that inoculation with *Bacillus* sp. wp-6 increased shoot and root fresh weights by 19% and 18%, respectively, after 40 days. The expression levels of alpha-linolenic acid metabolism-related proteins and metabolites (lipoxygenase 2, allene oxide synthase 2, jasmonic acid, 17-hydroxylinolenic acid) and flavonoid biosynthesis-related proteins and metabolites (chalcone synthase 2 and PHC 4′-O-glucoside) were up-regulated. In addition, the expression levels of amino acid metabolism-related proteins (NADH-dependent glutamate synthase, bifunctional aspartokinase/homoserine, anthranilate synthase alpha subunit 1, and 3-phosphoshikimate 1-carboxyvinyltransferase) and metabolites (L-aspartate, L-arginine, and *S*-glutathionyl-L-cysteine) were also significantly up-regulated. Among them, NADH-dependent glutamate synthase and bifunctional aspartokinase/homoserine could act as regulators of nitrogen metabolism. Overall, inoculation of wheat with *Bacillus* sp. wp-6 altered alpha-linolenic acid metabolism, amino acid metabolism, and flavonoid synthesis and promoted wheat seedling growth. This study will deepen our understanding of the mechanism by which *Bacillus* sp. wp-6 promotes wheat growth using proteomics and metabolomics.

Keywords Omics technologies · Plant growth-promoting rhizobacteria · Inoculation · Promoting wheat seedling growth

Introduction

The use of pesticides and chemical fertilizers in agricultural production has caused a series of environmental problems such as heavy metal pollution, so plant growth-promoting rhizobacteria (PGPR) has received more and more attention in recent years (Recep et al. 2009; Wang et al. 2020; Balasubramanian et al. 2021; Essalimi et al. 2022). Many studies have demonstrated that PGPR could positively impact plant hosts such as wheat (Ahmed et al. 2022), rice (Wiggins et al. 2022), *Arabidopsis thaliana* (Chu et al. 2020), potato (Recep et al. 2009), and tobacco (Zhang and Kong 2014). For example, inoculation with *Pseudomonas* PS01 could increase the root and shoot fresh weights of *Arabidopsis thaliana* seedlings (Chu et al. 2020). In addition, inoculation with *Bacillus* sp. ZH16 also could improve the morphology and ionic balance of wheat root, and increase plant nutrient content (Ahmed et al. 2022). This is because PGPR cannot only provide nutrients for plant growth, but also act as a biocontrol agent against pathogenic microorganisms (Trinh et al. 2018; Essalimi et al. 2022). For example, some studies found that PGPR could transform insoluble phosphorus and iron into soluble forms (Mushtaq et al. 2022), release phytohormones such as indoleacetic acid (Miljaković et al. 2022), and fix nitrogen in the soil (Tirry et al. 2021). Besides, PGPR could suppress the growth of

Communicated by Prakash Lakshmanan.

✉ Fenghua Zhang
zhangfenghua6088@126.com

[1] Key Laboratory of Oasis Ecological Agriculture of Xinjiang Production and Construction Corps, Shihezi University, North 4th Street No. 221, Shihezi 832003, Xinjiang, China

[2] Institute of Agriculture, School of Agriculture and Environment, The University of Western Australia, 35 Stirling Highway, Crawley, Perth, WA 6001, Australia

pathogenic microbes such as *Aspergillus niger* (Yuttavanichakul et al. 2012), *Armillaria* sp. (Ajilogba et al. 2016), and *Fusarium.* sp. (Cao et al. 2018). Therefore, PGPR has been widely used in agricultural production in recent years (Balasubramanian et al. 2021).

Plant–microbial interactions that promote plant growth have been the subject of numerous studies in recent years (Li et al. 2022). The studies of the physiological, genetic, and protein responses of plants inoculated with PGPR improve our understanding of the mechanisms of by which PGPR promotes plant growth (Ahmadi et al. 2013; Singh et al. 2017; Safdarian et al. 2019). For example, Elías et al. (2018) found that *Azospirillum brasilense* REC3 promoted strawberry growth by up-regulating genes related to ET signaling and indole-3-acetic acid (IAA) biosynthesis. Singh et al. (2017) also found that PGPR inoculation could promote the synthesis of defense enzymes and lignin in wheat, which improved wheat tolerance to abiotic stress. In addition, Kwon et al. (2016) reported that inoculation with *Pseudomonas polymyxa* E681 could promote *Arabidopsis thaliana* growth by up-regulating the expression of metabolism- and defense-related proteins. To date, modern "omics" technology combined with bioinformatics opens a new way for exploring the mechanisms of plant–microbial interactions (Rane et al. 2022). Especially, advances in proteomics and metabolomics technologies have proven to be an effective tool in providing insights into specific mechanisms of plant–microbe interactions (Rane et al. 2022). For example, proteomic and metabonomic analysis has shown that strain TJ6 inoculation could reduce Cd and Pb uptake in wheat through its own adsorption of Cd and Pb and regulation of DNA repair ability, plant hormone levels, and antioxidant activities of wheat root (Han et al. 2021).

In our previous studies, we found that the growth of wheat seedlings could be promoted by inoculation with *Bacillus* sp. wp-6 (Table S1). In this study, proteomic and metabolomic were combined to further investigate the growth-promoting effects of inoculation with *Bacillus* sp. wp-6 on wheat seedling growth. We hypothesize that (i) some proteins and metabolites that regulate wheat seedling growth and disease resistance after inoculation with *Bacillus* sp. wp-6, and (ii) there are regulatory relationships between these proteins and metabolites in different metabolic pathways to promote the growth of wheat seedlings. This study will deepen our understanding of the mechanism by which wp-6 promotes wheat growth, and contribute to the development of sustainable agriculture.

Materials and methods

Materials and experimental design

Bacillus sp. wp-6 was isolated from cotton grown in saline soil with an GenBank accession number MK 610676.1, and its characters are shown in Table S2.

Bacillus sp. wp-6 was incubated in 200 mL Luria–Bertani (LB) medium for 72 h, followed by centrifugation at 15,000 rpm at 4 °C for 1 min. After that, the supernatant was removed, then bacteria were re-suspended in sterile distilled water. Finally, the bacterial suspension was adjusted to a concentration of 10^8 CFU mL^{-1} using sterile distilled water.

Wheat seeds (variety Xinchun 5) were surface sterilized using 3% sodium hypochlorite for 5 min and rinsed five times with sterilized distilled water. The sterilized seeds were transferred to germinating box with three layers of filter paper at the bottom and germinated at 28 °C in the dark for 48 h. Three germinated seeds were planted in each presterilized plastic pot with 300 g non-autoclave potting soil (N: 50 mg L^{-1}, P: 30 mg L^{-1}, K: 60 mg L^{-1}, pH: 5.6, and electrical conductivity: 0.38 mS/cm). The treatments included (1) control, wheat seedlings were irrigated with 200 mL sterile distilled water every 3 days; (2) PGPR treatment, wheat seedlings were irrigated with 200 mL bacterial suspension (10^8 CFU mL^{-1}) every 3 days. Each treatment had five replicates (five pots). The pots were cultured in an incubator with a humidity of 30% and a 16-h light/8-h dark cycle at 28 °C. After 40 days, the plants were harvested and rhizosphere soil were carefully removed. Shoot fresh weight and root fresh weight were recorded. Then, shoot leaves were randomly selected (three from every pot) from each pot for proteomic and metabolomic analyses.

Protein extraction and protein digestion

Total protein extraction was performed using trichloroacetic acid (TCA)–acetone precipitation method as detailed by Wang et al. (2003). Fresh leave samples (0.5 g) were ground with liquid N_2 and transferred in 10 mL centrifugal tube containing 0.9 M sucrose, 0.5 M Tris–HCl, ethylenediaminetetraacetic acid, 0.1 M KCl, and 1% dithiothreitol (DTT). The suspension was sonicated in chilled acetone containing 10% (v/v) TCA and vortexed for 10 min. The mixture was centrifuged at 18,000 rpm at 4 °C for 15 min, and the supernatant was removed. The pellet were washed three times with pre-cooling acetone. Finally, the protein pellet was dried completely before dissolving in 50 mM ammonium bicarbonate with 1%

sodium dodecyl sulfate (SDS). Protein concentration was determined using the method of Bradford (Bradford 1976). Protein solution (100 µg) was used for trypsin (5.0 µg) digestion at 37 °C for 12 h.

Data-independent acquisition (DIA) mass spectrometry analysis

The peptides were separated using an Easy-nLC connected to a Q Exactive mass spectrometer (Thermo Fisher Scientific, San Jose, CA) with an increasing flow rate. The sample (1 µg) was injected on a self-made analytical column (75 µm inner diameter, 30 cm in length) packed with 3 µm Magic C18AQ medium (Bruker) at 50 °C. The flow rate was 300 nL min^{-1}, and the following linear gradient was used: 5–35% ACN with 0.1% formic acid for 2 h; 35–98% ACN for 2 min; 98% CAN for 8 min. For the data-dependent acquisition (DDA) analysis, the operating parameters of mass spectrometry were as follows: ion-source voltage: 1.6 kV; MS scan range: 350–1500 *m/z*; MS resolution: 60,000; automatic gain control (AGC): 3E6; maximum injection time: 50 ms; higher energy collisional dissociation mass spectrometry (HCD-MS/MS) resolution: 30,000; AGC: 1E5; maximum injection time: 100 ms; dynamic rejection time: 30 s; intensity threshold: 10,000; normalized collision energy (NCE): 28. For the DIA analysis, the operating parameters of mass spectrometry were as follows: ion-source voltage: 1.6 kV; MS scan range: 350–1500 *m/z*; MS resolution: 60,000; AGC: 3E6; maximum injection time: 50 ms; HCD–MS/MS resolution: 30,000; AGC: 1E5; maximum injection time: 100 ms; dynamic rejection time: 30 s; intensity threshold: 10,000; normalized collision energy (NCE): 22.5/25/27.5. DIA was performed with a variable isolation window. Each window overlapped 1 *m/z*. The 350–1500 Da was equally divided into 40 windows.

The DDA MS data were processed and analyzed using Max Quant (www.maxquant.org, version 1.5.1.2) (Cox et al. 2011). MS data were searched against the UniProtKB database (https://www.uniprot.org/uniprot/) spiked in protein consisted with 11 iRT peptide sequences. Trypsin was selected as digesting enzyme. The maximal two missed cleavage sites and the mass tolerance of 4.5 ppm for precursor ions and 20 ppm for fragment ions were defined for database search. Carbamidomethylation of cysteines was defined as fixed modification, while acetylation of protein n-terminal, oxidation of methionine was set as variable modifications for database searching. The identified peptides with a false discovery rate (FDR) ≤ 1% were used to construct a spectral library by the software Spectronaut (version 14.0, Biognosys). The DIA MS data were processed and analyzed with Spectronaut based on the constructed spectral library. The Spectronaut search were set as the default settings and the dynamic iRT was used for retention time prediction. The interference correction for MS/MS scan was enabled. The results were exported with FDR ≤ 1% at peptide level. Then, the mProphet algorithm was used to complete analytical quality control. The significant quantitative data were obtained through the R Bioconductor library (http://bioconductor.org/packages). The differentially expressed proteins (DEPs) were screened based on the threshold of fold-change > 2.0 or < 0.5 and adj_*p* value < 0.05.

Metabolite extraction and derivatization

Metabolites were extracted using the method detailed by Weckwerth et al. (2004). Leaf sample (0.5 g) were ground in liquid nitrogen, and the powder was transferred to a tube containing 0.75 mL of extraction buffer (methanol:chloroform:water = 5:2:2, v/v/v). Then, 5 µL 2-chloro-l-phenylalanine (initial concentration: 1 mg mL^{-1} in methanol, v/v) was added to each tube as the internal standard (final concentration: 0.02 mg mL^{-1}), and the mixture was vortexed for 60 s at 4 °C for 5 min. Ultrasonic crushing was performed at room temperature for 30 min, followed by placed at 4 °C for 10 min, and then centrifuged at 6000 rpm at 4 °C or 2 min. The supernatants (200 µL) was collected from each tube.

Liquid chromatograph–mass spectrometry (LC/MS) analysis

Liquid chromatograph–mass spectrometry (LC/MS) analysis was performed using an ultra-performance liquid chromatography (UPLC) system (Waters, UK). A reverse-phase T3 column (100 mm × 2.1 mm, 1.8 µm, Waters, UK) was used for separation of analytes. The mobile phase contained solvent A (water + 0.1% formic acid) and solvent B (methanol + 0.1% formic acid). The flow rate was 0.4 ml min^{-1}. Gradient elution conditions were set as follows: 0–2 min, 100% phase A; 2–11 min, 0% to 100% phase B; 11–13 min, 100% phase B; 13–15 min, 0–100% phase A. The sample (5 µL) was injected into the volume. A high-resolution tandem mass spectrometer (Xevo G2 XS QTOF, Waters, UK) scanning was operated in both positive and negative ion modes. For positive ion mode, the capillary voltage and sampling cone voltages were maintained at 3.0 kV and 40 V, respectively. For negative ion mode, the capillary voltage and sampling cone voltages were maintained at 2.0 kV and 40 V, respectively. The mass range was recorded from 50 to 1200 Da. The mass spectrometry data were acquired in Centroid MSE mode. During the acquisition, the LE signal was taken every 3 s to calibrate the mass accuracy. Furthermore, a quality control sample (pool of all samples) was use to evaluate the stability of the LC–MS.

Data preprocessing

Raw mass spectra were collected in continuum mode and processed using UNIFI (version 1.8, Waters, UK). Retention time was 0.5–18 min and the peak width was 1–30 s. The raw MS data were converted to MzXML files using ProteoWizard MSConvert software (http://proteowizard.sourceforge.net, version 3.0) and processed using Progenesis QI software (version 2.2, Waters, UK) for feature detection, retention time correction and alignment. QC-8 samples were used to standardize the data. Metabolite identification was performed based on accurate mass and product ion spectrum matching against KEGG database. Mass error was set to 5 ppm for first-search metabolite. A one-way ANOVA (Student's *t* test, Bonferroni-corrections) was use to identify significant differences between *Bacillus* sp. wp-6-inoculated wheat and control, and to calculate *p* values. The differential expressed metabolites (DEMs) were screened based on the threshold of fold-change > 1.5 or < 0.67 and *p* value < 0.05.

Bioinformatics analysis

To determine the functional characteristics of the identified proteins, Gene Ontology (GO) functional annotations and enrichment analysis were carried out using Blast2GO (http://blast2go.com/b2glaunch/resources). In addition, the classification and biological pathway of the DEPs and DEMs were performed using the online Kyoto Encyclopedia of Genes and Genomes (KEGG, http://www.kegg.jp/). The DEPs were assigned to eukaryotic orthologous groups (KOGs) database (ftp://ftp.ncbi.nih.gov/pub/COG/KOG/).

Statistical analysis

Statistical differences were determined by one-way ANOVA analysis using SPSS statistical software (version 22.0, IBM, Armonk, NY, USA). The mean differences were compared using Duncan's test ($p < 0.05$). The figures were made using Origin software (version 9.1, OriginLab, Hampton, MA, USA) and R software package (https://www.r-project.org/, version 4.0.0). Pearson correlations were carried out using R software package. The coefficients $|r| > 0.9$ and $p < 0.05$ were considered as significant correlations and used to construct networks using Cytoscape5 software (http://www.cytoscape.org/, version 3.2.1).

Results

Effect of *Bacillus* sp. wp-6 inoculation on wheat seedling growth

The inoculation with *Bacillus* sp. wp-6 obviously promoted wheat seedling growth (Fig. 1A). In addition, inoculation of *Bacillus* sp. wp-6 showed increases in shoot and root fresh weights by 19.72% and 18.18%, respectively ($p < 0.05$) (Fig. 1B, C).

Proteomic analysis of wheat seedlings in response to *Bacillus* sp. wp-6

To investigate the changes of protein profiles in mechanisms of wheat seedling in response to *Bacillus* sp. wp-6, protein profile analysis of wheat seedling leaves was performed. The identified peptides and proteins are shown in Table S3. A total of 78 proteins were differentially regulated ($p < 0.05$). Among these proteins, 59 proteins were up-regulated and 19 proteins were down-regulated (Table S4).

A total of 78 DEPs were categorized into cellular component (CC), biological processes (BP), and molecular function (MF) in the GO analysis (Fig. 2A). For the BP category, the most abundant groups included "metabolic process" and "cellular process". In the CC category, "cell" and "cell part" were the most represented groups. In the MF category, "catalytic activity" and "binding" were the most abundant groups. Among the 16 KOG categories, "General function prediction only" was the largest, followed by "Posttranslational modification, protein turnover, chaperones" and "Translation, ribosomal structure and biogenesis" (Fig. 2B). Among the 14 KEGG classification, global and overview maps was the most abundant groups, followed by carbohydrate metabolism and translation (Fig. 3A). Furthermore, all the DEPs were mapped to KEGG pathways by using *Brachypodium distachyon* as the model species. A total of 78 DEPs were enriched in 28 pathways (Table S5). The significant enrichment pathways were as followings ($p < 0.05$): biosynthesis of secondary metabolites, biosynthesis of amino acids, alpha-linolenic acid metabolism, porphyrin and chlorophyll metabolism, phenylalanine, tyrosine and tryptophan biosynthesis, metabolic pathways, pentose and glucuronate interconversions, monobactam biosynthesis, and linoleic acid metabolism (Fig. 3B). These results show that proteins involved in the synthesis of metabolites regulate various metabolic pathways in response to *Bacillus* sp. wp-6.

Metabonomic analysis of wheat seedlings in response to *Bacillus* sp. wp-6

A total of 78 DEPs involved in various cellular metabolism pathway through proteomics analysis. To investigate

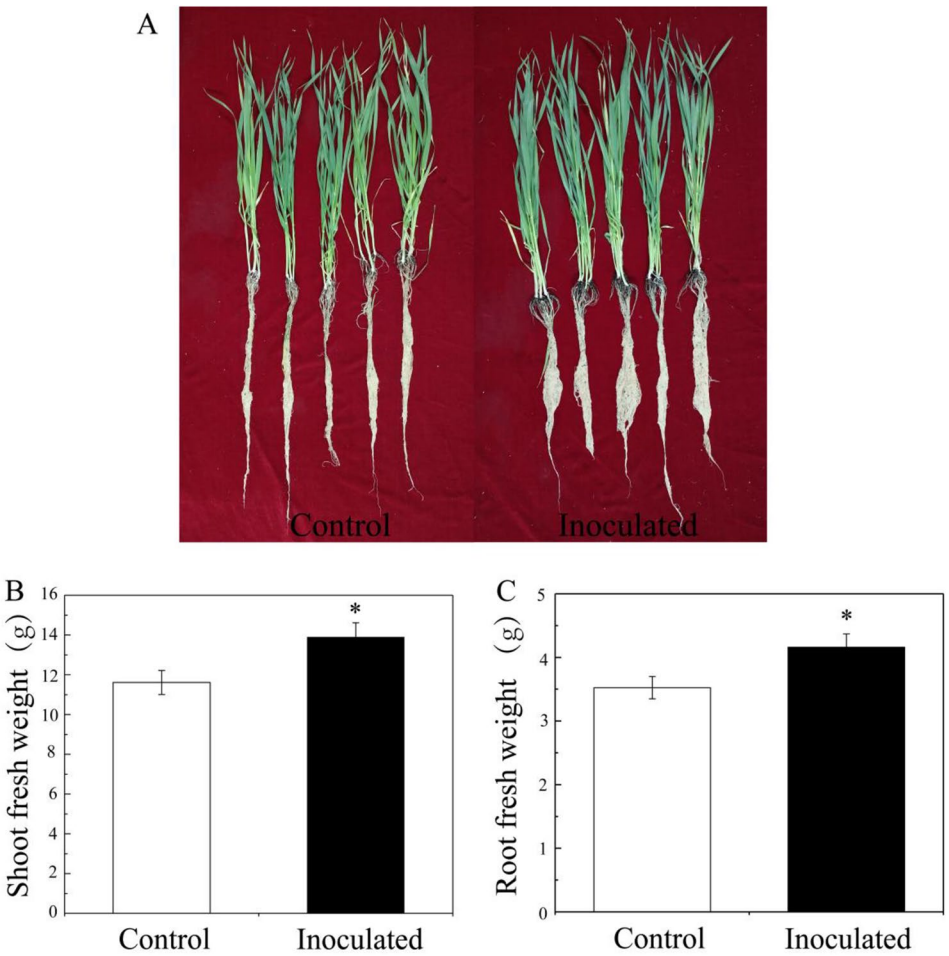

Fig. 1 Effect of *Bacillus* sp. wp-6 inoculation on the growth of wheat seedling ($n = 5$, 3 plants per pot). Photograph of wheat seedlings (**A**), shoot fresh weight (**B**), and root fresh weight (**C**) of wheat seed after 40 days of wp-6 inoculation. Data represent the means ± SEM of five replicates. The asterisk indicate significant difference ($p < 0.05$) among different treatments. "Control" represents non-inoculated wheat plants, "Inoculated" represents inoculated wheat plants

changes in the related metabolic processes, we conducted a hierarchical cluster analysis based on the DEMs in each group of samples (Fig. 4A). There was a clear separation of metabolites between *Bacillus* sp. wp-6-inoculated and non-inoculated wheat seedling. In addition, a total of 68 metabolites were up-regulated and 37 were down-regulated (Table S6).

Furthermore, all the DEMs were mapped to KEGG pathways using *Brachypodium distachyon* as the model species. A total of 105 DEMs were enriched in 38 pathways (Table S7). The significant enrichment pathways were as followings ($p < 0.05$): flavone and flavonol biosynthesis, benzoxazinoid biosynthesis, ABC transporters, arginine biosynthesis, phenylalanine metabolism, vitamin B6 metabolism, monobactam biosynthesis, alpha-linolenic acid metabolism, cyanoamino acid metabolism, aminoacyl-tRNA biosynthesis, cysteine and methionine metabolism (Fig. 4B). The changes in these metabolites and metabolic pathways provide important information on how wheat seedling responds to *Bacillus* sp. wp-6.

Integrative proteomic and metabonomic analyses of wheat seedlings inoculated with *Bacillus* sp. wp-6

To integrate the results of proteomics and metabolomics analyses, a KEGG mapping was performed based on the DEPs and the DEMs. A total of 11 metabolic pathways showed changes in *Bacillus* sp. wp-6-inoculated wheat seedling plants, including biosynthesis of secondary metabolites, biosynthesis of amino acids, alpha-linolenic acid metabolism, metabolic pathways, monobactam biosynthesis, lysine biosynthesis, flavonoid biosynthesis, alanine, aspartate and glutamate metabolism, glycine, serine and threonine metabolism, cysteine and methionine metabolism, and carbon metabolism (Table S8).

To better observe the relationship between these important pathways, we constructed a comprehensive systemic metabolic pathway diagram by combining the KEGG pathways of Table 1. As shown in Fig. 5, eight proteins and five metabolites were mapped into the diagram. It was found that the expressions of LOX2 (2.28-fold), AOS2 (2.02-fold),

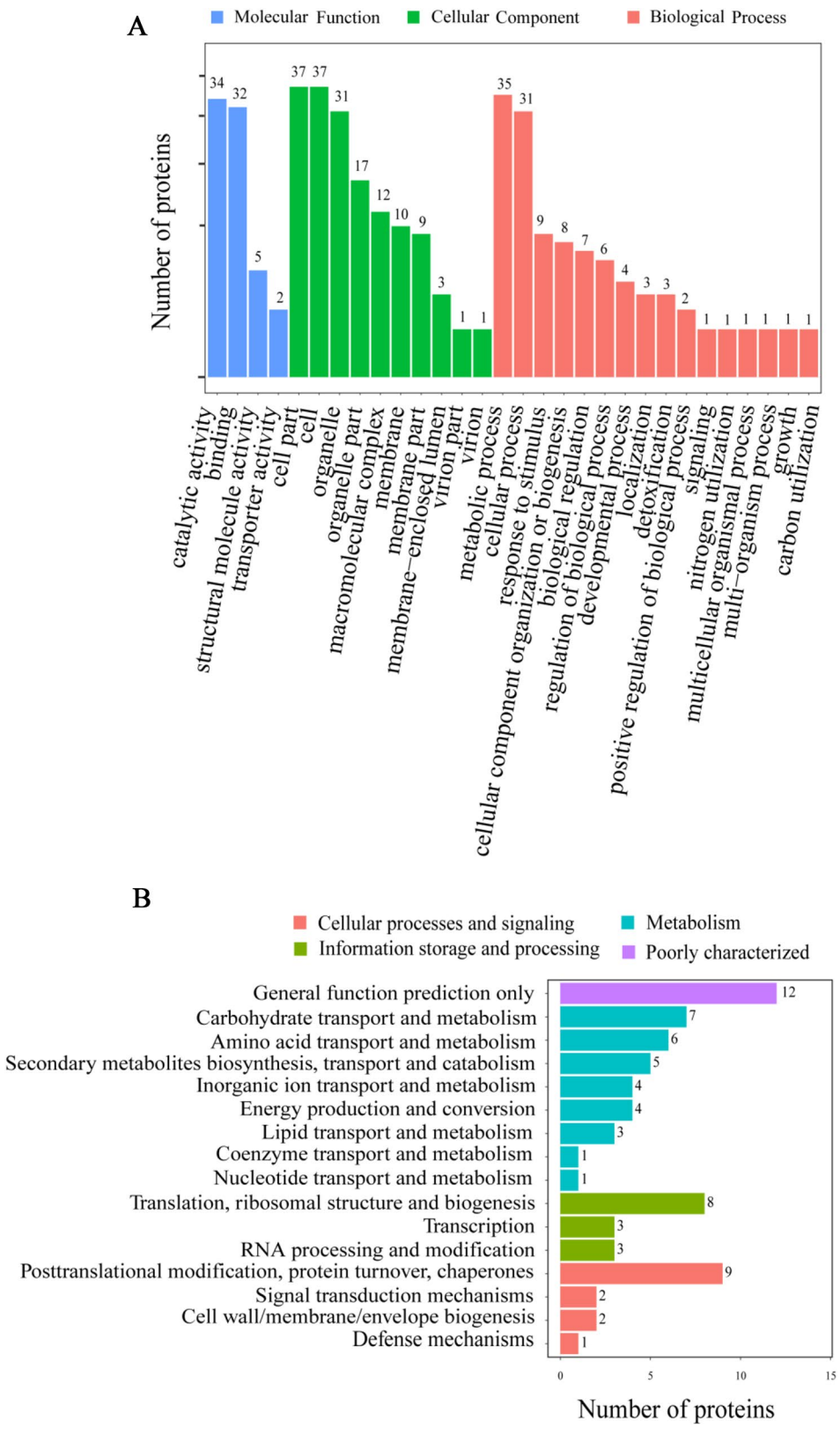

Fig. 2 **A** GO classification of the identified proteins in *Bacillus* sp. wp-6-inoculated versus non-inoculated wheat plants. The results for the three main GO categories are summarized: BP, CC, and MF, **B** KOG annotation of the differentially expressed proteins in *Bacillus* sp. wp-6-inoculated versus non-inoculated wheat plants

(−)-jasmonic acid (2.01-fold), and 17-hydroxylinolenic acid (2.23-fold) were up-regulated in the alpha-linolenic acid metabolism (Table 2). In addition, the expressions of NADH-GOGAT, AKHSDH2, ASA1, At2g45300, L-aspartate, L-arginine, and *S*-glutathionyl-L-cysteine in biosynthesis of amino acids and alanine, aspartate and glutamate

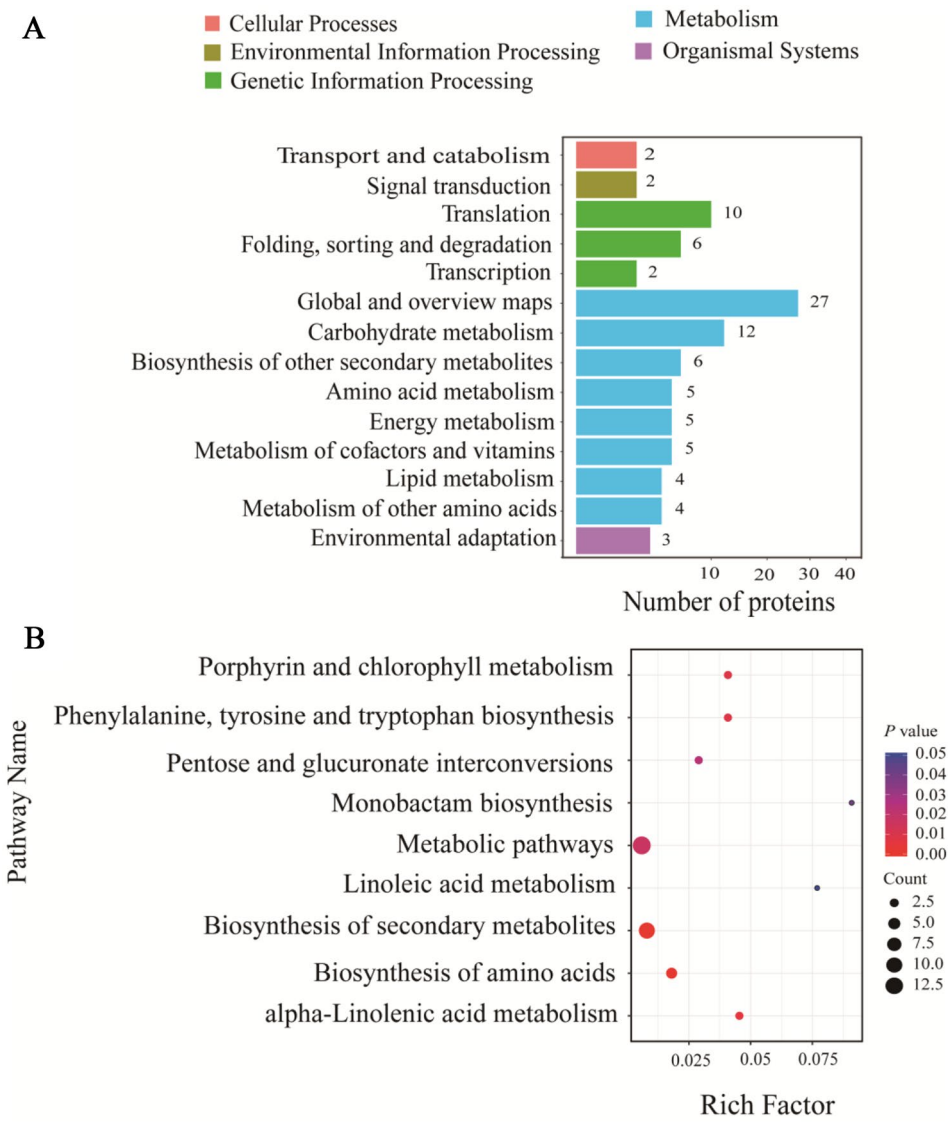

Fig. 3 **A** KEGG classification of the differentially expressed proteins involved in the response to *Bacillus* sp. wp-6 in the leaves of wheat, **B** KEGG pathways of the differentially expressed proteins involved in the response to *Bacillus* sp. wp-6 in the leaves of wheat

metabolism were up-regulated, and 2.71-fold, 2.62-fold, 2.97-fold, 2.03-fold, 1.53-fold, 1.75-fold, and 1.61-fold changes were detected, respectively (Table 3). AKHSDH2, L-aspartate, and *S*-glutathionyl-L-cysteine are involved in glycine, serine and threonine metabolism, lysine biosynthesis, and cysteine and methionine metabolism. The expression of GLO3 was down-regulated and that of L-aspartate was up-regulated in the carbon metabolism. The expressions of CHS2 (2.62-fold) and PHC 4′-O-glucoside (1.56-fold) in flavonoid biosynthesis were up-regulated (Table 4).

To further reveal the regulatory effect of *Bacillus* sp. wp-6 on the metabolism of wheat seedlings, the correlation network diagram was constructed based on the DEPs and DEMs in 11 common pathways (Fig. 6). It was found that L-aspartate was positively correlated with AOS2, LOX2, AKHSDH2, NADH-GOGAT, At2g45300, ASA1, and CHS2 ($|r| > 0.9$, $p < 0.05$), but negatively correlated with GLO3 ($|r| > 0.9$, $p < 0.05$). L-Arginine was positively correlated with AOS2, LOX2, AKHSDH2, NADH-GOGAT, At2g45300, ASA1, and CHS2 ($|r| > 0.9$, $p < 0.05$). Like L-aspartate, but negatively correlated with GLO3 ($|r| > 0.9$, $p < 0.05$). Jasmonic acid and 17-hydroxylinolenic acid were positively correlated with AOS2, AKHSDH2, At2g45300, ASA1, and CHS2 ($|r| > 0.9$, $p < 0.05$). In addition, the jasmonic acid was also positively correlated with LOX2 and NADH-GOGAT ($|r| > 0.9$, $p < 0.05$). PHC 4′-O-glucoside and *S*-glutathionyl-L-cysteine were positively correlated with LOX2, AKHSDH2, NADH-GOGAT, At2g45300, ASA1, and CHS2 ($|r| > 0.9$, $p < 0.05$). The above results show that *Bacillus* sp. wp-6 has a potential regulatory relationship in promoting the growth of wheat seedlings.

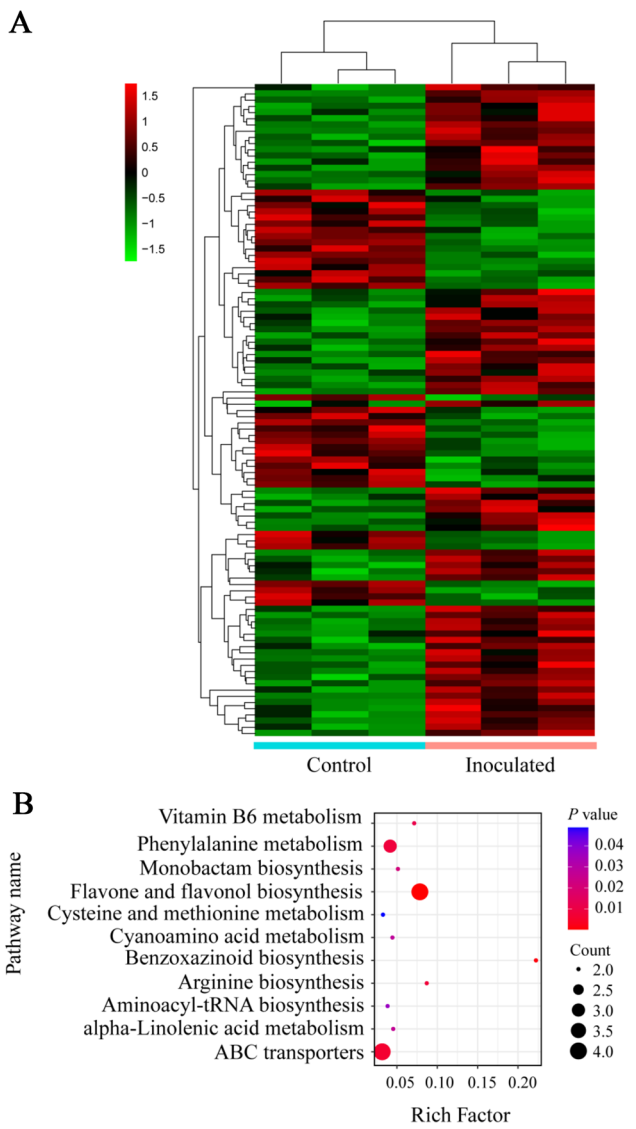

Fig. 4 **A** Hierarchical cluster heat map of different metabolites in *Bacillus* sp. wp-6-inoculated versus non-inoculated wheat plants; **B** KEGG pathways of the different metabolites involved in the response to *Bacillus* sp. wp-6 in the leaves of wheat. "Control" represents non-inoculated wheat plants, "Inoculated" represents inoculated wheat plants

Discussion

Effects of *Bacillus* sp. wp-6 inoculation on the growth of wheat seedlings

Plant growth-promoting rhizobacteria (PGPR) can promote plant growth through a variety of mechanisms such as solubilizing insoluble mineral constituents and suppressing the growth of pathogenic microorganisms (Kwon et al. 2016; Shen et al. 2022; Liu et al. 2022). In this study, *Bacillus* sp. wp-6 could secrete IAA and produce siderophores and solubilize phosphorus (Table S1). Indole-3-acetic acid (IAA) is a plant hormone which can promote plant growth (Wang et al. 2015; Chu et al. 2020). For example, Miljaković et al. (2022) found that inoculation with *Bacillus megaterium,* which could secrete IAA, increased root and shoot dry weights of soybean seedlings. Siderophore-producing microbes could promote plant growth via iron chelation and indirectly suppress the growth of plant pathogenic fungi (Olanrewaju and Babalola 2022). For example, siderophore-producing *Acinetobacter calcoaceticus* improved the iron concentration and overall plant growth of potato (Mushtaq et al. 2022). In addition, a consequential reduction in pathogenicity in banana plants was noted through inoculating with siderophore-producing *Bacillus siamensis* (Shen et al. 2022). Phosphorus-solubilizing microorganisms could mineralise unavailable organic phosphorus to available, which promotes the absorption of phosphorus for plant growth (Tu et al. 2022). For example, Di et al. (2022) found that *Bacillus subtilis* B9 inoculation could promote sugarcane seedlings to uptake more phosphorus. Hence, *Bacillus* sp. wp-6 could secreted IAA, produce siderophore, and improve the ability of dissolving phosphorus, which resulted in enhanced plant growth.

Alpha-linolenic acid metabolism

Alpha-linolenic acid can inhibit innate immunity responses related to callose deposition in wheat (Ren et al. 2022). In addition, the proteins and metabolites involved in the metabolism of alpha-linolenic acid, such as lipoxygenase (LOX), allene oxide synthase (AOS), 12-oxo-phytodienoic acid reductase (OPR), and jasmonic acid (JA), are also important for plants' defense against biotic and abiotic stresses (Fernandes and Ghag 2022; Fu et al. 2022; Li et al. 2020). In this study, inoculation with *Bacillus* sp. wp-6 induced a significant up-regulation of LOX2 and AOS2 in wheat seedling leaves (Fig. 5, Table 2). Similar results were also observed in other studies in which AOS and LOX were up-regulated in wheat root inoculated with *Bacillus velezensis* (Kang et al. 2019*)*. Dong et al. (2022) also reported that AOS and LOX were induced after the inoculation of beneficial strain F1-35 in the watermelons. Allene oxide synthase (AOS), a cytochrome P450 enzyme of the CYP74A family, which is a major control point of JA signaling in potato (Gorina et al. 2022). Kazerooni et al. (2022) have found that AOS overexpression can promotes JA biosynthesis to prevent damage caused by pathogens. Like AOS, LOX can also indirectly prevent plant diseases by regulating JA biosynthesis (Wang et al. 2022a). For example, inoculation with *Paenibacillus sp.* strain B2 and *Arthrobacter* spp. strain AA induced the accumulation of JA in wheat plants through the up-regulation of AOS and LOX, whereas JA prevented the

Table 1 Proteins and metabolites involved in common pathways

Pathway name	Proteomics		Metabolomics	
	Pathway ID	*p* value	Pathway ID	*p* value
Biosynthesis of secondary metabolites	bdi01110	0.00728	bdi01100	0.1605322
Biosynthesis of amino acids	bdi01230	0.00815	bdi01230	0.1695389
Alpha-linolenic acid metabolism	bdi00592	0.0114	bdi00592	0.02681243
Metabolic pathways	bdi01100	0.0212	bdi01100	0.8769291
Monobactam biosynthesis	bdi00261	0.0405	bdi00261	0.02139734
Lysine biosynthesis	bdi00300	0.0584	bdi00300	0.1840171
Flavonoid biosynthesis	bdi00941	0.163	bdi00941	0.349765
Alanine, aspartate and glutamate metabolism	bdi00250	0.178	bdi00250	0.178
Glycine, serine and threonine metabolism	bdi00260	0.215	bdi00260	0.2522118
Cysteine and methionine metabolism	bdi00270	0.326	bdi00270	0.0486977
Carbon metabolism	bdi01200	0.603	bdi01200	0.4790615

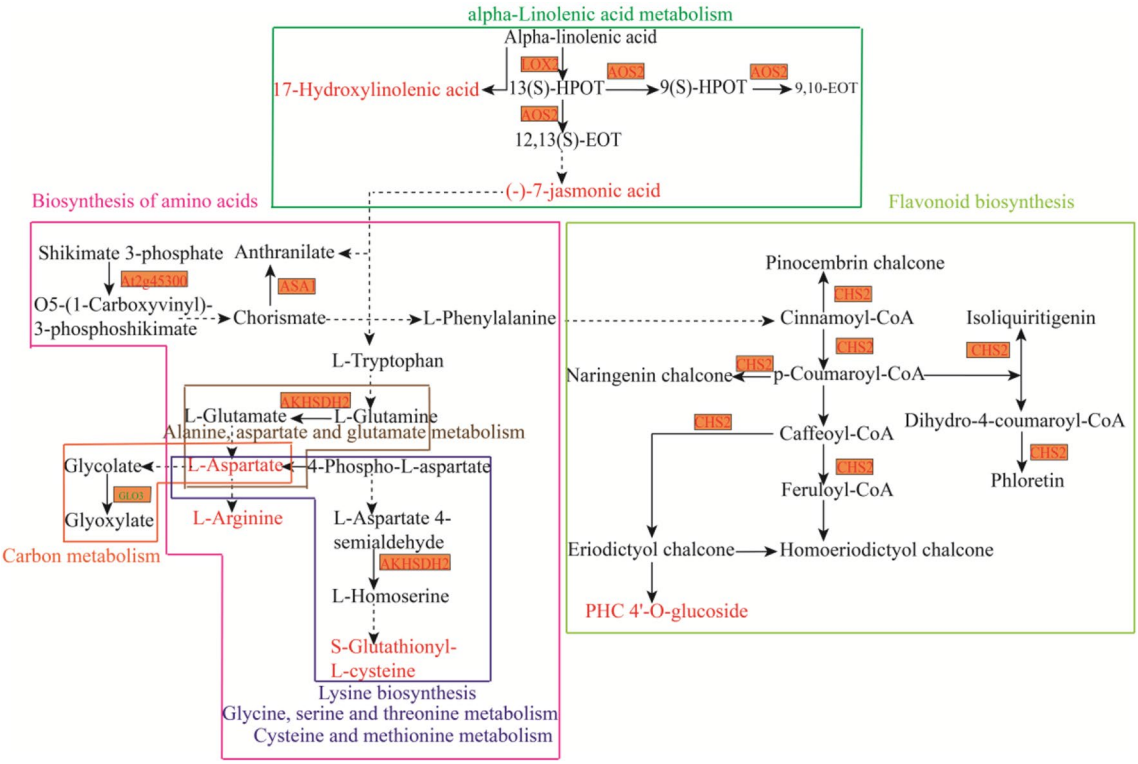

Fig. 5 Proteins (boxes) and metabolites (arrows) were mapped to a comprehensive systemic metabolic pathways diagram by combining the KEGG pathways of the DEMs and DEPs. Red indicates up-regulation; green indicates downregulation. The solid lines indicate direct interactions, while the dashed lines indicate effects mediated by additional molecules

pathogenic fungus (*Zymoseptoria tritici*) (Samain et al. 2022). Our metabolome analysis results also showed that inoculation with *Bacillus* sp. wp-6 induced a significant accumulation of JA in wheat seedling leaves (Table 2). In addition, this study also found JA was highly positively correlated with the proteins AOS and LOX (Fig. 6). This result further confirmed that up-regulation of AOS and LOX promoted JA synthesis in wheat seedling leaves. Similar studies found that the accumulation of *Bacillus subtilis*-induced JA can activate tomato plants to produce induced systemic resistance (ISR) and protect plants from pathogens (Veselova et al. 2022). Taken together these findings provide evidence that inoculation with *Bacillus* sp. wp-6 can promote JA accumulation by stimulating the expression of LOX2 and AOS2 proteins to protect wheat seedlings from pathogen infection.

Table 2 Alpha-linolenic acid metabolism-related proteins and metabolites in common pathway

Accession	Gene name	Protein name	Fold change	adj_p value
Proteins				
A0A3B6HS52	AOS2	Allene oxide synthase 2	2.28	0.000
A0A3B6MID4	LOX2	Lipoxygenase 2	2.02	0.002
Metabolite	Adducts	Mass Error	Fold change	*p* value
Metabolites				
(−)-7-Jasmonic acid	M+FA−H	−4.2048	2.01	0.029
17-Hydroxylinolenic acid	$M-H_2O-H$	−2.9480	2.23	0.024

Table 3 Amino acid metabolism-related proteins and metabolites in common pathway

Accession	Gene name	Protein name	Fold change	adj_*p* value
Proteins				
A0A3B6FNM9	NADH-GOGAT	NADH-dependent glutamate synthase	2.71	0.008
A0A3B6KHC1	AKHSDH2	Bifunctional aspartokinase/homoserine dehydrogenase 2	2.62	0.002
A0A3B6LVK5	ASA1	Anthranilate synthase alpha subunit 1	2.97	0.009
A0A3B6TCN7	At2g45300	3-Phosphoshikimate 1-Carboxyvinyltransferase	2.03	0.007
Metabolite	Adducts	Mass error	Fold change	*p* value
Metabolites				
L-Aspartate	$M+H-H_2O$, M+H, M+Na	2.586	1.53	0.004
L-Arginine	M+H	−4.850	1.75	0.002
S-Glutathionyl-L-cysteine	M+H	1.327	1.61	0.017

Table 4 Flavonoid biosynthesis-related proteins and metabolites in common pathway

Accession	Gene name	Protein name	Fold change	adj_*p* value
Proteins				
A0A1U9Y670	CHS2	Chalcone synthase 2	2.62	0.001
Metabolite	Adducts	Mass error	Fold change	*p* value
Metabolites				
PHC 4'-O-glucoside	M+Na	3.261976	1.56	0.030

Amino acid metabolism

Amino acids are involved in plant's protein synthesis, signal transduction, and growth (Qian et al. 2022). In addition, the metabolites produced during the metabolism of amino acids are also essential for plant growth and defense against various stresses (Reddy et al. 2022). Wang et al. (2022b) showed that an increase in amino acids metabolism of cucumber by *Bacillus velezensis* SX13 inoculation. Almuhayawi et al. (2021) also found *Streptomyces* (strain JSA11) inoculation could promote the accumulation of amino acids in *Chenopodium*. Our study obtained similar results. We found that the expression levels of amino acids metabolism-related the proteins and metabolites including NADH-GOGAT, AKHSDH2, ASA1, At2g45300, L-aspartate, and L-arginine were up-regulated (Fig. 5, Table 3). Previous studies have shown that NADH-GOGAT and AKHSDH2 play important roles in nitrogen metabolism (Huang et al. 2022b; Liang et al. 2022). For example, the increased expression of NADH-GOGAT in rice roots enhanced primary assimilation of $NH4^+$, which further promoted nitrogen metabolism (Yamaya and Kusano 2014). Bifunctional aspartokinase/homoserine dehydrogenase 2 (AKHSDH2) could promote the conversion of aspartic acid to aspartate family amino

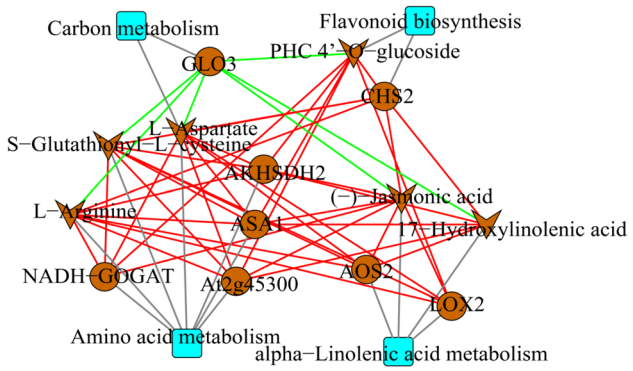

Fig. 6 Correlation network analysis of the differentially expressed proteins and metabolites. The red line represents a positive correlation between the differential metabolites and the differential proteins; the green line represents a negative correlation; the grey represents the differential metabolites and the differential proteins belong to this pathway

acids, which is a part of the coordinated regulatory mechanism of nitrogen and carbon storage, and utilization (Liang et al. 2022). In this study, we found L-aspartate and L-arginine were positively correlated with AKHSDH2 and NADH-GOGAT (Fig. 6). In addition, our results also found that inoculation with *Bacillus* sp. wp-6 promoted the accumulation of L-aspartate and L-arginine in wheat seedlings (Fig. 5, Table 3). L-Aspartate and L-arginine are used for nitrogen storage and transport in many plants (Conesa et al. 2022). For example, in tomato, genes involved in plant resistance to infectious pathogens are up-regulated with changes in nitrogen levels (Vega et al. 2015). Meanwhile, increasing nitrogen levels also can provide additional nutrients to support the growth of plant (Reddy et al. 2022). Hence, nitrogen metabolism not only affects plant growth but also plays an important role in plant defense (Reddy et al. 2022). ASA1 and At2g45300 play important roles in the biosynthesis of phenylalanine, tyrosine and tryptophan (Lou et al. 2022). Many studies have shown that the metabolism of phenylalanine, tyrosine and tryptophan produces a large number of secondary metabolites, such as lignins, phytoalexins, and alkaloids (Huang et al. 2022a; Abdelaziz et al. 2022). Besides, studies have also found that ASA1 and At2g45300 can mediate the synthesis of secondary metabolites to prevent pathogen infection in barley and maize (Hu et al. 2009; Abdelaziz et al. 2022). This study found that the expression of ASA1 and At2g45300 were up-regulated after *Bacillus* sp. wp-6 inoculation (Fig. 5, Table 3). These results indicate that *Bacillus* sp. wp-6 inoculation could provide additional nutrients for wheat and defense against pathogens through improving nitrogen metabolism, thus promoting wheat growth.

Flavonoid biosynthesis

Flavonoids are a group of polyphenol secondary metabolites, which play variable and species-dependent roles in plant defenses (Liu et al. 2022). For example, flavonoids can protect bilberry from a pathogen (*Botrytis cinerea*) (Parvandi et al. 2021). In this study, we found that flavonoid biosynthesis-related proteins and metabolites, such as CHS2 and PHC 4′-O-glucoside, were up-regulated (Fig. 5, Table 4). Similar studies also reported that the expression of CHS gene in rice was up-regulated by inoculated with *Herbaspirillum seropedicae* (Wiggins et al. 2022). Chalcone synthase (CHS) is a key enzyme in the biosynthesis of flavonoids. The increased expression levels of CHS2 gene can protect ginger from infection by *Fusarium solani* (Zhou et al. 2022). In addition, El-Gendi et al. (2022) have shown that the overexpression of CHS2 gene in tobacco plants promoted flavonoid accumulation. In this study, we found PHC 4′-O-glucoside was highly positively correlated with the protein CHS2 in flavonoid biosynthesis (Fig. 6). In addition, our metabolome analysis results showed that PHC 4′-O-glucoside was up-regulated in wheat seedlings inoculated with *Bacillus* sp. wp-6 (Table 4). Begum et al. (2022) have confirmed that the flavonoids content in tobacco plants could be increased by inoculation with *Bacillus methylotrophicus*. However, the accumulation of flavonoid could be used by plants to prevent pathogen infection after they break through the plant's constructive defense system (Liu et al. 2022). Hence, inoculation with *Bacillus* sp. wp-6 protects wheat seedlings from pathogen infection by promoting flavonoid biosynthesis, thus promoting wheat growth.

Table 5 Carbon metabolism-related proteins and metabolites in common pathway

Accession	Gene name	Protein name	Fold change	adj_*p* value
Proteins				
A0A3B6CD34	GLO3	Peroxisomal (S)-2-hydroxy-acid oxidase	0.39	0.000
Metabolite	Adducts	Mass error	Fold change	*p* value
Metabolites				
L-Aspartate	M+H−H_2O, M+H, M+Na	2.586	1.53	0.004

Carbon metabolism

One-carbon (C1) unit is essential for plants, and its metabolism can provide energy for plant growth (Kołton et al. 2022). In this study, our results found that inoculation with *Bacillus* sp. wp-6 promoted the accumulation of L-aspartate in wheat seedlings (Fig. 5, Table 5). Studies have shown that L-aspartate is vital for nitrogen storage and transport in many plants, and plays an important role in nitrogen metabolism (Conesa et al. 2022). (*S*)-2-Hydroxy-acid oxidase (GLO3), a photorespiration enzyme, which greatly impact plants' photosynthesis in plant (Yu et al. 2018). However, in this study, GLO3 was down-regulated in carbon metabolism (Fig. 5, Table 5). In addition, the metabolites L-aspartate and L-arginine had were negatively correlated with GLO3 (Fig. 6). This phenomenon might be caused by a decrease in the energy consumption of carbon metabolism and an increase in energy supplies for amino acid metabolism.

Conclusions

In summary, inoculation with *Bacillus* sp. wp-6 induced the accumulation of JA signaling molecules in wheat seedlings through the up-regulation of AOS and LOX, whereas JA triggered the ISR to protect wheat seedlings from pathogen infection (Fig. 7). Besides, it also promoted amino acid metabolism by up-regulating proteins (ASA1, At2g45300, NADH-GOGAT, and AKHSDH2) and metabolites (L-aspartate and L-arginine). Nitrogen metabolism could provide additional nutrients for wheat seedlings and defense against pathogens. The up-regulation of proteins (NADH-GOGAT and AKHSDH2), and accumulation of metabolites (L-aspartate and L-arginine) could promote nitrogen metabolism through regulating amino acid metabolism. The up-regulation of proteins ASA1 and At2g45300 in amino acid metabolism can mediate the flavonoid biosynthesis to prevent pathogen infection in wheat seedlings. In addition, amino acid metabolism has a negative feedback effect on carbon metabolism. These results provide a comprehensive understanding of the mechanism by which inoculation with *Bacillus* sp. wp-6 promotes wheat seedling growth. Overall, this research shows the application potential of *Bacillus* sp. wp-6 in sustainable agricultural development.

In future, *Bacillus* sp. wp-6 can be widely used to replace the agrochemicals such as chemical fertilizers and pesticides in sustainable agricultural production. However, many issues still need to be resolved before *Bacillus* sp. wp-6 can be widely used. For instance, this research was conducted in the greenhouse and laboratory conditions. Therefore, it is necessary to explore the effects of *Bacillus* sp. wp-6 inoculation in the field. Besides, the massive production of this strain to meet the requirements of large-scale field use also requires new technologies. Moreover, the application of single strain wp-6 in different crop production practices is very limited. Therefore, the use of multiple strains might be more effective for the production of different crops in sustainable agriculture.

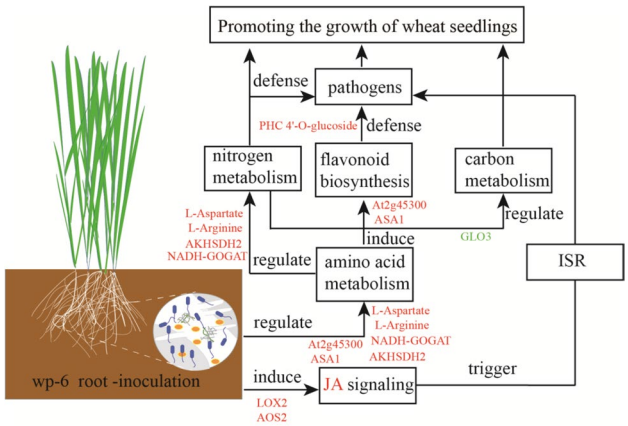

Fig. 7 Proposed model of the growth promotion and defense response in wheat seedling caused by *Bacillus* sp. wp-6 inoculation. Red indicates up-regulation; green indicates downregulation

Author contribution statement

YGZ and FHZ designed and carried out the experiment. YGZ collected the data. YGZ performed the analysis. YGZ, FHZ, and DW analyzed the results. YGZ wrote the manuscript. YGZ, FHZ, and BM checked and revised the final version of the manuscript.

Supplementary Information The online version contains supplementary material available at https://doi.org/10.1007/s00299-022-02947-x.

Funding This research was financially supported by the National Natural Science Foundation of China (Grant No. 31860360) and the Science and Technology Cooperation Project of Xinjiang (Grant No. 2020BC001).

Availability of data and materials Not applicable.

Declarations

Conflict of interest The authors declare that they have no competing interests.

Consent to participate Not applicable.

Consent to publish We certify that the submission is not under review at any other publication.

References

Abdelaziz AM, El-Wakil DA, Attia MS, Ali OM, AbdElgawad H, Hashem AH (2022) Inhibition of *Aspergillus flavus* growth and

aflatoxin production in *Zea mays* L. using endophytic *Aspergillus fumigatus*. J Fungi 8:482. https://doi.org/10.3390/jof8050482
Ahmadi J, Asgharzadeh A, Bakhtiari S (2013) The effect of microbial inoculants on physiological responses of two wheat cultivars under salt stress. Int J Adv Biol Biomed Res 4:364–371
Ahmed T, Noman M, Rizwan M, Ali S, Ijaz U, Nazir MM, ALHaithloul HAZ, Alghanem SM, Li B, (2022) Green molybdenum nanoparticles-mediated bio-stimulation of *Bacillus* sp. strain ZH16 improved the wheat growth by managing in planta nutrients supply, ionic homeostasis and arsenic accumulation. J Hazard Mater 423:127024. https://doi.org/10.1016/j.jhazmat.2021.127024
Ajilogba C, Babalola O, Adebola P, Adeleke R (2016) Evaluation of PGPR and biocontrol activities of bacteria isolated from Bambara groundnut rhizosphere. New Biotechnol 2016:S128–S129. https://doi.org/10.1016/j.nbt.2016.06.1169
Almuhayawi MS, Abdel-Mawgoud M, Al Jaouni SK, Almuhayawi SM, Alruhaili MH, Selim S, AbdElgawad H (2021) Bacterial endophytes as a promising approach to enhance the growth and accumulation of bioactive metabolites of three species of *Chenopodium* sprouts. Plants 10:2745. https://doi.org/10.3390/plants10122745
Balasubramanian VK, Dampanaboina L, Cobos CJ, Yuan N, Xin Z, Mendu V (2021) Induced secretion system mutation alters rhizosphere bacterial composition in *Sorghum bicolor* (L.) Moench. Planta 253:1–18. https://doi.org/10.1007/s00425-021-03569-5
Begum N, Wang L, Ahmad H, Akhtar K, Roy R, Khan MI, Zhao T (2022) Co-inoculation of arbuscular mycorrhizal fungi and the plant growth-promoting rhizobacteria improve growth and photosynthesis in tobacco under drought stress by up-regulating antioxidant and mineral nutrition metabolism. Microb Ecol 83:971–988. https://doi.org/10.1007/s00248-021-01815-7
Bradford MM (1976) A rapid and sensitive method for the quantitation of microgram quantities of protein utilizing the principle of protein-dye binding. Anal Biochem 72:248–254. https://doi.org/10.1016/0003-2697(76)90527-3
Cao Y, Pi HL, Chandrangsu P, Li YT, Wang YQ, Zhou H, Xiong HQ, Helmann JD, Cai YF (2018) Antagonism of two plant-growth promoting *Bacillus velezensis* isolates against *Ralstonia solanacearum* and *Fusarium oxysporum*. Sci Rep 8:1–14. https://doi.org/10.1038/s41598-018-22782-z
Chu TN, Bui LV, Hoang MTT (2020) *Pseudomonas* PS01 isolated from maize rhizosphere alters root system architecture and promotes plant growth. Microorganisms 8:471
Conesa MR, Conejero W, Vera J, Ruiz-Sánchez M (2022) Root reserves ascertain postharvest sensitivity to water deficit of nectarine trees. Agronomy 12:1805. https://doi.org/10.3390/agronomy12081805
Cox J, Michalski A, Mann M (2011) Software lock mass by two-dimensional minimization of peptide mass errors. J Am Soc Mass Spectr 22:1373–1380. https://doi.org/10.1007/s13361-011-0142-8
Di YN, Kui L, Singh P, Liu LF, Xie LY, He LL, Li FS (2022) Identification and characterization of *Bacillus subtilis* B9: a diazotrophic plant growth-promoting endophytic bacterium isolated from sugarcane root. J Plant Growth Regul. https://doi.org/10.1007/s00344-022-10653-x
Dong XM, Lian QG, Chen J, Jia RM, Zong ZF, Ma Q, Wang Y (2022) The improved biocontrol agent, F1–35, protects watermelon against *Fusarium* Wilt by triggering jasmonic acid and ethylene pathways. Microorganisms 10:1710. https://doi.org/10.3390/microorganisms10091710
El-Gendi H, Al-Askar AA, Király L, Samy MA, Moawad H, Abdelkhalek A (2022) Foliar Applications of *Bacillus subtilis* HA1 culture filtrate enhance tomato growth and induce systemic resistance against tobacco mosaic virus infection. Horticulturae 8:301. https://doi.org/10.3390/horticulturae8040301
Elías JM, Guerrero-Molina MF, Martínez-Zamora MG, Díaz-Ricci JC, Pedraza RO (2018) Role of ethylene and related gene expression in the interaction between strawberry plants and the plant growth-promoting bacterium *Azospirillum brasilense*. Plant Biol 20:490–496. https://doi.org/10.1111/plb.12697
Essalimi B, Esserti S, Rifai LA, Koussa T, Makroum K, Belfaiza M, Rifai S, Venisse JS, Faize L, Alburquerque N, Burgos L, Jadoumi SE, Faize M (2022) Enhancement of plant growth, acclimatization, salt stress tolerance and verticillium wilt disease resistance using plant growth-promoting rhizobacteria (PGPR) associated with plum trees (*Prunus domestica*). Sci Hortic 291:110621. https://doi.org/10.1016/j.scienta.2021.110621
Fernandes LB, Ghag SB (2022) Molecular insights into the jasmonate signaling and associated defense responses against wilt caused by *Fusarium oxysporum*. Plant Physiol Biochem 174:22–34. https://doi.org/10.1016/j.plaphy.2022.01.032
Fu J, Ren R, Jin S, Fang R, Wen Z, Yang M, Wang X, Liu B, Yin T, Lu G, Yang Y, Qi J (2022) Overexpression of a putative 12-oxophytodienoate reductase gene, EpOPR1, enhances acetylshikonin production in *Echium plantagineum*. In Vitro Cell Dev Biol Plant 58:311–320. https://doi.org/10.1007/s11627-022-10259-8
Gorina S, Ogorodnikova A, Mukhtarova L, Toporkova Y (2022) Gene expression analysis of potato (*Solanum tuberosum* L.) lipoxygenase cascade and oxylipin signature under abiotic stress. Plants 11:683. https://doi.org/10.3390/plants11050683
Han H, Zhang H, Qin S, Zhang J, Yao L, Chen Z, Yang J (2021) Mechanisms of *Enterobacter bugandensis* TJ6 immobilization of heavy metals and inhibition of Cd and Pb uptake by wheat based on metabolomics and proteomics. Chemosphere 276:130157. https://doi.org/10.1016/j.chemosphere.2021.130157
Hu P, Meng Y, Wise RP (2009) Functional contribution of chorismate synthase, anthranilate synthase, and chorismate mutase to penetration resistance in barley–powdery mildew interactions. Mol Plant Microbe Interact 22:311–320. https://doi.org/10.1094/MPMI-22-3-0311
Huang S, Lim SY, Lau H, Ni W, Li SFY (2022a) Effect of glycinebetaine on metabolite profiles of cold-stored strawberry revealed by 1H NMR-based metabolomics. Food Chem 393:133452. https://doi.org/10.1016/j.foodchem.2022.133452
Huang XJ, Jian SF, Chen DL, Zhong C, Miao JH (2022b) Concentration-dependent dual effects of exogenous sucrose on nitrogen metabolism in *Andrographis paniculata*. Sci Rep 12:1–11. https://doi.org/10.1038/s41598-022-08971-x
Kang X, Wang L, Guo Y, ul Arifeen MZ, Cai X, Xue Y, Bu Y, Wang G, Liu C (2019) A comparative transcriptomic and proteomic analysis of hexaploid wheat's responses to colonization by *Bacillus velezensis* and *Gaeumannomyces graminis*, both separately and combined. Mol Plant Microbe Interact 32:1336–1347. https://doi.org/10.1094/MPMI-03-19-0066-R
Kazerooni EA, Maharachchikumbura SS, Al-Sadi AM, Rashid U, Kim ID, Kang SM, Lee IJ (2022) Effects of the rhizosphere fungus *Cunninghamella bertholletiae* on the *Solanum lycopersicum* response to diverse abiotic stresses. Int J Mol Sci 23:8909. https://doi.org/10.3390/ijms23168909
Kołton A, Długosz-Grochowska O, Wojciechowska R, Czaja M (2022) Biosynthesis regulation of folates and phenols in plants. Sci Hortic 291:110561. https://doi.org/10.1016/j.scienta.2021.110561
Kwon YS, Lee DY, Rakwal R, Baek SB, Lee JH, Kwak YS, Seo JS, Chung WS, Bae DW, Kim SG (2016) Proteomic analyses of the interaction between the plant-growth promoting rhizobacterium *Paenibacillus polymyxa* E681 and *Arabidopsis thaliana*. Proteomics 16:122–135. https://doi.org/10.1002/pmic.201500196
Li Y, Qiu L, Liu X, Zhang Q, Zhuansun X, Fahima T, Sun Q, Krugman T, Xie C (2020) Glycerol-induced powdery mildew resistance in wheat by regulating plant fatty acid metabolism, plant hormones cross-talk, and pathogenesis-related genes. Int J Mol Sci 21:673. https://doi.org/10.3390/ijms21020673

Li YH, Yang YY, Wang ZG, Chen Z (2022) Emerging function of ecotype-specific splicing in the recruitment of commensal microbiome. Int J Mol Sci 23:4860. https://doi.org/10.3390/ijms23094860

Liang X, Deng H, Bai Y, Fan TP, Zheng X, Cai Y (2022) Characterization of a novel type homoserine dehydrogenase with high oxidation activity from *Arthrobacter nicotinovorans*. Process Biochem 114:102–110. https://doi.org/10.1016/j.procbio.2022.01.019

Liu Y, Gao S, Zhang Y, Zhang Z, Wang Q, Xu Y, Wei J (2022) Transcriptomics and metabolomics analyses reveal defensive responses and flavonoid biosynthesis of *Dracaena cochinchinensis* (Lour.) S. C. Chen under wound stress in natural conditions. Molecules 27:4514. https://doi.org/10.3390/molecules27144514

Lou H, Yang Y, Zheng S, Ma Z, Chen W, Yu C, Song L, Wu J (2022) Identification of key genes contributing to amino acid biosynthesis in Torreya grandis using transcriptome and metabolome analysis. Food Chem 379:132078. https://doi.org/10.1016/j.foodchem.2022.132078

Miljaković D, Marinković J, Tamindžić G, Đorđević V, Tintor B, Milošević D, Ignjatov M, Nikolić Z (2022) Bio-priming of soybean with *Bradyrhizobium japonicum* and *Bacillus megaterium*: strategy to improve seed germination and the initial seedling growth. Plants 11:1927. https://doi.org/10.3390/plants11151927

Mushtaq Z, Asghar HN, Zahir ZA, Maqsood M (2022) The interactive approach of rhizobacteria and l-tryptophan on growth, physiology, tuber characteristics, and iron concentration of potato (*Solanum tuberosum* L.). J Plant Growth Regul 41:1359–1366

Olanrewaju OS, Babalola OO (2022) The rhizosphere microbial complex in plant health: a review of interaction dynamics. J Integr Agric 21:2168–2182. https://doi.org/10.1016/S2095-3119(21)63817-0

Parvandi M, Rezadoost H, Farzaneh M (2021) Introducing *Alternaria tenuissima* SBUp1, as an endophytic fungus of Ferula assa-foetida from Iran, which is a rich source of rosmarinic acid. Lett Appl Microbiol 73:569–578. https://doi.org/10.1111/lam.13542

Qian R, Hu Q, Ma X, Zhang X, Ye Y, Liu H, Gao H, Zheng J (2022) Comparative transcriptome analysis of heat stress responses of *Clematis lanuginosa* and *Clematis crassifolia*. BMC Plant Biol 22:1–16. https://doi.org/10.1186/s12870-022-03497-w

Rane NR, Tapase S, Kanojia A, Watharkar A, Salama ES, Jang M, Yadav KK, Amin MA, Cabral-Pinto MMS, Jadhav JP, Jeon BH (2022) Molecular insights into plant–microbe interactions for sustainable remediation of contaminated environment. Bioresour Technol 344:126246. https://doi.org/10.1016/j.biortech.2021.126246

Recep K, Fikrettin S, Erkol D, Cafer E (2009) Biological control of the potato dry rot caused by *Fusarium* species using PGPR strains. Biol Control 50:194–198. https://doi.org/10.1016/j.biocontrol.2009.04.004

Reddy DP, Pal A, Reddy MD (2022) Effect of nitrogen levels on yield of rice varieties during kharif in South Odisha. Crop Res 57:108–112. https://doi.org/10.31830/2454-1761.2022.015

Ren J, Zhang Y, Wang Y, Li C, Bian Z, Zhang X, Liu H, Xu J, Jiang C (2022) Deletion of all three MAP kinase genes results in severe defects in stress responses and pathogenesis in *Fusarium graminearum*. Stress Biol 2:1–13. https://doi.org/10.1007/s44154-021-00025-y

Safdarian M, Askari H, Shariati V, Nematzadeh G (2019) Transcriptional responses of wheat roots inoculated with *Arthrobacter nitroguajacolicus* to salt stress. Sci Rep 9:1–12. https://doi.org/10.1038/s41598-018-38398-2

Samain E, Ernenwein C, Aussenac T, Selim S (2022) Effective and durable systemic wheat-induced resistance by a plant-growth-promoting rhizobacteria consortium of *Paenibacillus* sp. strain B2 and *Arthrobacter* spp. strain AA against *Zymoseptoria tritici* and drought stress. Physiol Mol Plant Pathol 119:101830. https://doi.org/10.1016/j.pmpp.2022.101830

Shen N, Li S, Li S, Zhang H, Jiang M (2022) The siderophore-producing bacterium, *Bacillus siamensis* Gxun-6, has an antifungal activity against *Fusarium oxysporum* and promotes the growth of banana. Egypt J Biol Pest Control 32:1–9. https://doi.org/10.1186/s41938-022-00533-7

Singh RP, Runthala A, Khan S, Jha PN (2017) Quantitative proteomics analysis reveals the tolerance of wheat to salt stress in response to *Enterobacter cloacae* SBP-8. PLoS One 12:e0183513. https://doi.org/10.1371/journal.pone.0183513

Tirry N, Kouchou A, El Omari B, Ferioun M, El Ghachtouli N (2021) Improved chromium tolerance of *Medicago sativa* by plant growth-promoting rhizobacteria (PGPR). J Genet Eng Biotechnol 19:1–14. https://doi.org/10.1186/s43141-021-00254-8

Trinh CS, Lee H, Lee WJ, Lee SJ, Chung N, Han J, Kim J, Hong S, Lee H et al (2018) Evaluation of the plant growth-promoting activity of *Pseudomonas nitroreducens* in *Arabidopsis thaliana* and *Lactuca sativa*. Plant Cell Rep 37:873–885. https://doi.org/10.1007/s00299-018-2275-8

Tu C, Jin Z, Che F, Cao X, Song X, Lu C, Huang W (2022) Characterization of phosphorus sorption and microbial community in lake sediments during overwinter and recruitment periods of cyanobacteria. Chemosphere 307:135777. https://doi.org/10.1016/j.chemosphere.2022.135777

Vega A, Canessa P, Hoppe G, Retamal I, Moyano TC, Canales J, Gutiérrez RA, Rubilar J (2015) Transcriptome analysis reveals regulatory networks underlying differential susceptibility to *Botrytis cinerea* in response to nitrogen availability in *Solanum lycopersicum*. Front Plant Sci 6:911. https://doi.org/10.3389/fpls.2015.00911

Veselova SV, Sorokan AV, Burkhanova GF, Rumyantsev SD, Cherepanova EA, Alekseev VY, Sarvarova ER, Kasimova AR, Maksimov IV (2022) By modulating the hormonal balance and ribonuclease activity of tomato plants *Bacillus subtilis* induces defense response against potato virus X and potato virus Y. Biomolecules 12:288. https://doi.org/10.3390/biom12020288

Wang W, Scali M, Vignani R, Spadafora A, Sensi E, Mazzuca S, Cresti M (2003) Protein extraction for two-dimensional electrophoresis from olive leaf, a plant tissue containing high levels of interfering compounds. Electrophoresis 24:2369–2375. https://doi.org/10.1002/elps.200305500

Wang J, Zhang Y, Li Y, Wang X, Nan W, Hu Y, Zhang H, Zhao C, Wang F, Li P, Shi H, Bi Y (2015) Endophytic microbes *Bacillus* sp. LZR216-regulated root development is dependent on polar auxin transport in *Arabidopsis* seedlings. Plant Cell Rep 34:1075–1087. https://doi.org/10.1007/s00299-015-1766-0

Wang A, Hua J, Wang Y, Zhang G, Luo S (2020) Stereoisomers of nonvolatile acetylbutanediol metabolites produced by *Bacillus velezensis* WRN031 improved root elongation of maize and rice. J Agr Food Chem 68:6308–6315. https://doi.org/10.1021/acs.jafc.0c01352

Wang C, Zhang M, Zhou J, Gao X, Zhu S, Yuan L, Hou X, Liu T, Chen G, Tang X, Shan G, Hou J (2022a) Transcriptome analysis and differential gene expression profiling of wucai (*Brassica campestris* L.) in response to cold stress. BMC Genom 23:1–16. https://doi.org/10.1186/s12864-022-08311-3

Wang J, Qu F, Liang J, Yang M, Hu X (2022b) *Bacillus velezensis* SX13 promoted cucumber growth and production by accelerating the absorption of nutrients and increasing plant photosynthetic metabolism. Sci Hortic 301:111151. https://doi.org/10.1016/j.scienta.2022.111151

Weckwerth W, Loureiro ME, Wenzel K, Fiehn O (2004) Differential metabolic networks unravel the effects of silent plant phenotypes. Proc Acad Sci USA 101:7809–7814. https://doi.org/10.1073/pnas.0303415101

Wiggins G, Thomas J, Rahmatallah Y, Deen C, Haynes A, Degon Z, Glazko G, Mukherjee A (2022) Common gene expression patterns are observed in rice roots during associations with plant growth-promoting bacteria, *Herbaspirillum seropedicae* and *Azospirillum brasilense*. Sci Rep 12:1–11. https://doi.org/10.1038/s41598-022-12285-3

Yamaya T, Kusano M (2014) Evidence supporting distinct functions of three cytosolic glutamine synthetases and two NADH-glutamate synthases in rice. J Exp Bot 65:5519–5525. https://doi.org/10.1093/jxb/eru103

Yu XL, Wu DM, Fu YQ, Yang XJ, Baluška F, Shen H (2018) OsGLO4 is involved in the formation of iron plaques on surface of rice roots grown under alternative wetting and drying condition. Plant Soil 423:111–123. https://doi.org/10.1007/s11104-017-3493-5

Yuttavanichakul W, Lawongsa P, Wongkaew S, Teaumroong N, Boonkerd N, Nomura N, Tittabutr P (2012) Improvement of peanut rhizobial inoculant by incorporation of plant growth promoting rhizobacteria (PGPR) as biocontrol against the seed borne fungus, *Aspergillus niger*. Biol Control 63:87–97. https://doi.org/10.1016/j.biocontrol.2012.06.008

Zhang CS, Kong FY (2014) Isolation and identification of potassium-solubilizing bacteria from tobacco rhizospheric soil and their effect on tobacco plants. Appl Soil Ecol 82:18–25. https://doi.org/10.1016/j.apsoil.2014.05.002

Zhou J, Liu X, Sun C, Li G, Yang P, Jia Q, Cai X, Zhu Y, Yin J, Liu Y (2022) Silica nanoparticles enhance the disease resistance of ginger to rhizome rot during postharvest storage. Nanomaterials 12:1418. https://doi.org/10.3390/nano12091418